Atmospheric Environment 45 (2011) 7379–7395

Contents lists available at ScienceDirect

Atmospheric Environment

journal homepage: www.elsevier.com/locate/atmosenv

The model SIRANE for atmospheric urban pollutant dispersion; part I, presentation of the model

Lionel Soulhac, Pietro Salizzoni*, F.-X. Cierco, Richard Perkins

Laboratoire de Mécanique des Fluides et d'Acoustique, UMR CNRS 5509, University of Lyon Ecole Centrale de Lyon, INSA Lyon, Université Claude Bernard Lyon I, 36, avenue Guy de Collongue, 69134 Ecully, France

ARTICLE INFO

Article history:
Received 15 February 2011
Received in revised form
22 June 2011
Accepted 4 July 2011

Keywords:
Numerical model
Pollutant dispersion
Street network
Urban canopy

ABSTRACT

In order to control and manage urban air quality, public authorities require an integrated approach that incorporates direct measurements and modelling of mean pollutant concentrations. These have to be performed by means of operational modelling tools, that simulate the transport of pollutants within and above the urban canopy over a large number of streets. The operational models must be able to assess rapidly a large variety of situations and with limited computing resources.

SIRANE is an operational urban dispersion model based on a simplified description of the urban geometry that adopts parametric relations for the pollutant transfer phenomena within and out of the urban canopy.

The streets in a city district are modelled as a network of connected street segments. The flow within each street is driven by the component of the external wind parallel to the street, and the pollutant is assumed to be uniformly mixed within the street. The model contains three main mechanisms for transport in and out of a street: advection along the street axis, diffusion across the interface between the street and the overlying air flow and exchanges with other streets at street intersections.

The dispersion of pollutants advected or diffused out of the streets is taken into account using a Gaussian plume model, with the standard deviations σ_y and σ_z parameterised by the similarity theory. The input data for the final model are the urban geometry, the meteorological parameters, the background concentration of pollutants advected into the model domain by the wind and the emissions within each street in the network.

1. Introduction

Environmental policies and legislation induce public authorities to adopt strategies to manage air pollution and to minimise its impact on human health and the environment. To accomplish these tasks it is necessary to have tools to characterise urban air pollution levels. For several years, in almost all European and North American cities, this characterisation mainly relied on the direct measurements of concentration of the different pollutant species. Nevertheless, even if these measurements provide direct information of the air pollution level at given positions, they do not provide an exhaustive picture of the distribution of air pollution throughout urban areas nor the possibility to evaluate the impact of a new traffic plan. For this reason, during the last decade, public authorities have increasingly adopted pollutant dispersion models to complement the information provided by monitoring networks.

Based on mathematical descriptions of the phenomena governing pollutant transport in the atmosphere, these models allow us to estimate the temporal and spatial evolution of air pollutants, providing essential information to estimate their impact on environment and human health.

Several modelling tools are available nowadays. However, given the wide range of phenomena and scales involved, it is not possible to model pollutant dispersion in the atmosphere with a unique model. A large variety of models have been therefore developed, depending on the length scales characterising the dispersion phenomena. Five characteristic scales are usually identified: the continental scale ($\sim$1000 km), the regional scale ($\sim$100 km), the urban scale ($\sim$10 km), the district scale ($\sim$1 km) and the street scale ($\sim$100 m). Within all these scales, the district scale is certainly the one that has been hitherto the least studied. However, this scale is the one that is mainly associated with the details needed to define pollutant cartographies in urban areas.

Pollutant dispersion modelling at the district scale must account for the modification to the atmospheric flow due to the presence of a city. As summarised by Roth (2000), the main effects are the

* Corresponding author.
E-mail address: pietro.salizzoni@ec-lyon.fr (P. Salizzoni).

1352-2310/$ – see front matter © 2011 Elsevier Ltd. All rights reserved.
doi:10.1016/j.atmosenv.2011.07.008

List of symbols

a	Albedo (–)
$C_{D,\mathrm{build}}$	Buildings drag coefficient (–)
Cld	Cloud coverage (octas)
C_p	Specific heat capacity at constant pressure of air ($C_p = 1005$ J kg^{-1} K^{-1})
C_{street}	Spatially averaged concentration in street canyons (kg m^{-3})
$C_{\mathrm{street,ext}}$	Concentration above roof level (kg m^{-3})
d_{district}	Displacement height of the district (m)
f	Coriolis parameter ($f = 4\pi\sin(2\pi\phi/360)/86{,}400$)
F_m	Momentum flux (m^4 s^{-2})
F_b	Buoyancy flux (m^4 s^{-3})
g	Gravitational acceleration ($g = 9.81$ m s^{-2})
h	Atmospheric boundary layer depth (m)
H	Street height (m)
H_0	Sensible heat flux between ground and atmosphere (W m^{-2})
H_{build}	Mean height of the streets (m)
H_s	Height of the source of pollutant (m)
$H_{s,\mathrm{eff}}$	Effective height of the source of pollutant (m)
ΔH	Plume rise (m)
k_1	Chemical reaction constant (s^{-1})
k_2	Chemical reaction constant (m^6 mol^{-2} s^{-1})
k_3	Chemical reaction constant (m^3 mol^{-1} s^{-1})
K_{turb}	Turbulent diffusivity (m^2 s^{-1})
L	Street length (m)
L_{MO}	Monin–Obukhov length (m)
N	Brunt–Vaïsälä frequency (s^{-1})
Pr	Precipitations intensity (mm h^{-1})
P_{street}	Air flux along the street (m^3 s^{-1})
P_{vert}	Vertical air flux within a street intersection (m^3 s^{-1})
Q_G	Heat flux in the ground (W m^{-2})
Q_E	Latent heat flux ground-atmosphere (W m^{-2})
Q_I	Pollutant flux entering in the street at the upwind intersection (kg s^{-1})
Q_{wash}	Wet deposition flux within the street (kg s^{-1})
$Q_{\mathrm{part,gr}}$	Dry deposition flux within the street (kg s^{-1})
Q_S	Pollutant flow rate at the source (kg s^{-1})
$Q_{S,\mathrm{eff}}$	Effective pollutant flow rate after wash-out (kg s^{-1})
R_N	Net radiation (W m^{-2})
T_0	Temperature at ground level (K)
T_a	Air temperature (K)
T_L	Lagrangian time scale (s)
u_*	Friction velocity (m s^{-1})
$u(z)$	Wind speed (m s^{-1})
u_d	Mass exchange velocity between street canyon and atmosphere (m s^{-1})
U_{ext}	Measured wind velocity (m s^{-1})
U_m	Plume advective velocity (m s^{-1})
U_{street}	Averaged wind velocity along the street axis (m s^{-1})
w_*	Convective velocity scale (m s^{-1})
W	Street width (m)
$z_{0,\mathrm{build}}$	Aerodynamic roughness of the street walls (m)
$z_{0,\mathrm{district}}$	Aerodynamic roughness of the district (m)
z_m	Averaged height of the pollutant plume (m)
z_T	Thermal roughness of the district (m)
$\theta(z)$	Potential temperature (K)
θ_0	Potential temperature at ground level (K)
θ_*	Friction temperature (K)
φ	Wind direction with respect to the street axis (degree)
ϕ	Site latitude (degree)
ψ_m, ψ_h	Businger universal functions
α	Priestley–Taylor coefficient (–)
ε	District emissivity (–)
$\gamma_\theta^{\mathrm{ext}}$	Vertical gradient of potential temperature in the atmosphere (K m^{-1})
κ	Von Karman constant ($\kappa = 0.4$)
λ_P	Obstacle density (–)
λ_F	Frontal obstacle density (–)
λ_{veg}	Rate of the surface covered by vegetation (–)
Λ	Wash-out rate (s^{-1})
χ	solar elevation (degree)
ν_a	Cinematic viscosity of the air (m^2 s^{-1})
ρ_a	Air density (kg m^{-3})
σ_v	Standard deviation of the transversal velocity (m s^{-1})
σ_w	Standard deviation of the vertical velocity (m s^{-1})
σ_φ	Standard deviation of the horizontal wind direction (degree)
ζ	NO_2 emission rate (–)

presence of intense shear layers at the top of the urban canopy, the wake diffusion induced by buildings which enhances turbulent transport of momentum, heat, moisture and pollutants and the drag induced by buildings. Furthermore, emission sources at this scale are particularly difficult to model, since they are due to inhomogeneous and unsteady traffic fluxes and other kind of distributed emissions, for example heating and industries. In order to model flow and dispersion phenomena at this scale two choices are then available:

- a complete reconstruction of the urban geometry within the computational domain and the solution of the system of the governing equations by means of computational fluid dynamics (CFD) codes;
- a simplified description of the urban geometry and a parametrisation of the mass and momentum transfer within and above the urban canopy.

The current hardware capabilities already allows the computation of wind fields for air quality modelling purposes over entire urban districts with CFD diagnostic models (e.g. Hanna et al., 2006; Flaherty et al., 2007; Singh et al., 2008) or with prognostic models (e.g. Trini Castelli et al., 2004; Duchenne and Armand, 2010).

However, when a district of hundreds of streets is considered and a large amount of the urban pollutant emissions has to be taken into account, the application of diagnostic and prognostic CFD codes requires computational costs that are still unfeasible for operational purposes.

An operational approach has therefore to be based on a simplified description of the urban geometry and on the pollutant transfer phenomena. This requires us to:

- characterise the lower part of the atmospheric boundary layer, where the flow dynamics are typically determined by the size and the density of the buildings and by the street geometry (Christen et al., 2007; Rotach, 1993; Kastner-Klein et al., 2004; Salizzoni et al., 2009a);
- estimate the advective pollutant fluxes along the street axis (Soulhac et al., 2008; Barlow et al., 2009);
- parameterise the mass exchange between the recirculating region within the street canyons and the external flow (Gomes et al., 2007; Cai et al., 2008; Salizzoni et al., 2009b);

- parameterise the mass exchange at street intersections (Soulhac et al., 2009; Tomlin et al., 2009; Carpintieri and Robins, 2010).

In the last twenty years few models for pollutant dispersion in an urban district have been developed. SBLINE (Namdeo and Colls, 1996) assumes that the pollutant in each street is due to the contribution of sources located in the street itself and those located in the surrounding streets. This is taken into account by a Gaussian model, assuming that the plume of pollutants is transported as if there were no buildings. The direct contribution of the street is computed with the model CPBM (Yamartino and Wiegand, 1986) which evaluates the mass exchanges at street intersections.

Similarly, ADMS-Urban (McHugh et al., 1997) provides a module to compute mean concentration in the regions of the domain where the street canyon effect arises. For each street canyon, the concentration is computed as the sum of two components: the background concentration due to street canyon trapping effect and the concentration related to the direct contribution of vehicles emissions within the street. The street canyon trapping effect is parameterised using the Danish Operational Street Pollution Model (Hertel and Berkowicz, 1989). This street canyon module is activated when the street aspect ratio between the averaged height H of the buildings bordering one street and its width W is larger than 0.5, otherwise pollutant concentration are determined from Gaussian plume distributions. The dispersion of pollutant emitted within the street is modelled by a Gaussian plume, whose lateral spreading is computed by specific relations for the turbulent fluctuations within the canyon.

The aim of developing a new modelling tool for pollutant dispersion at the district scale has motivated the long term research program undertaken at the Laboratoire de Mécanique des Fluides et Acoustique de l'Ecole Centrale de Lyon in the last fifteen years. The result of this work is a new pollutant dispersion model, named SIRANE. SIRANE adopts an approach different to the ADMS-Urban and SBLINE models. The model is based on the street network concept and on a decomposition of the whole flow into the external atmospheric and the urban canopy sub-flow.

The aim of this paper is to give a detailed presentation of the parametrisation adopted in the model. In the second part of this study (Soulhac et al., submitted for publication) we will present a validation of the model against field data.

2. Model outline

SIRANE is an urban pollutant dispersion model conceived to simulate pollutant dispersion emitted from line sources (e.g. traffic emissions) and point sources (e.g. chimneys) at the district scale, for typical length scales ranging from a few hundreds metres to few kilometres. SIRANE adopts a quasi-steady approximation. Typically, the time step is assumed to be equal to 1 h, as in almost all pollutant dispersion models. This choice is motivated by the spectral gap (Stull, 1988) between the time scale associated to the dynamic of atmospheric turbulence and that related to variation of the synoptic meteorological conditions. For each time step pollutant dispersion is computed assuming steady conditions and concentration are estimated independently from that in the previous time step, i.e. assuming no contribution of the pollutant emissions emitted previously. It is therefore evident that this approach reveals its limits in case of calm wind conditions persisting over several hours. This can induce a significant accumulation of pollutants over the urban area which will not be taken into account by the model.

The starting point of SIRANE is the decomposition of the domain in two sub domains, the external atmosphere and the urban canopy. Therefore the model is made up of two independent modules to compute flow and dispersion within the urban canopy and in the overlying atmospheric boundary layer.

The streets in a district are modelled as a simplified network (Fig. 1a) of connected street segments – represented by boxes. The flow within each street is driven by the parallel component of the external wind and the pollutant is assumed to be uniformly mixed over the volume of the street. In order to compute the mean concentration within each street, SIRANE accounts for three transport mechanisms within the canopy:

- Convective mass transfer along the street (Soulhac et al., 2008) due to the mean wind along their axis (Fig. 1b);

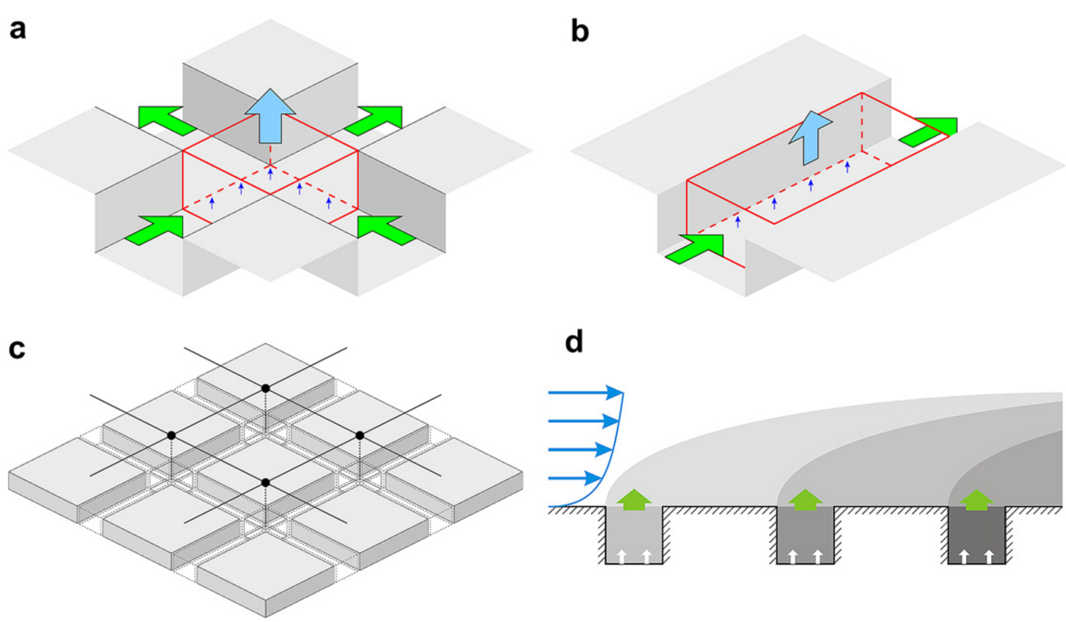

Fig. 1. The different components of the SIRANE model. (a) Modelling a district by a network of streets. (b) Box model for each street, with corresponding flux balance. (c) Fluxes at a street intersection. (d) Modified Gaussian plume for roof level transport.

- Turbulent transfer across the interface (Salizzoni et al., 2009a) between the street and the overlying atmospheric boundary layer (Fig. 1b);
- Convective transport at street intersections (Soulhac et al., 2009). Exchange ratios have been parameterised by a mass exchange tensor, which accounts for the influence of the external flow direction (Fig. 1c).

The flow above the street network is described by the Monin–Obukhov similarity theory. The presence of the roughness sub-layer just above the urban canopy is neglected and the external flow is assumed to be uniform in the horizontal plane. The dispersion of pollutants advected or diffused into the overlying air is taken into account using a Gaussian plume model (see Fig. 1d), with the standard deviations σ_y and σ_z parameterised by similarity theory.

In the following sections we describe the geometrical description of the domain (Section 3) and the parametrisations implemented in the model. These concern the flow and dispersion within the urban canopy (Section 4) and above roof level (Section 5). Then we present the models of the physico-chemical transformation adopted in SIRANE (Section 6) and the numerical methods adopted to solve the final system of linear equations (Section 7) Finally, we recall the main shortcomings of the model (Section 8) and we give an overview on the validation of SIRANE which have been performed so far (Section 9).

3. Geometrical description of the district

Pollutant dispersion at the district scale is influenced by the multitude of buildings in the district whose geometry must be taken into account in any model. The main difficulty is to find the compromise between the need for accurate description of the urban geometry, the minimisation of the costs of collection and management of cartographic data and highly resolved (in time and space) computations. The degree of simplification of the urban geometry which can be reasonably adopted for operational purposes must therefore be determined.

The real geometry of an urban district is characterised by three main length scales which act differently on pollutant dispersion patterns:

- *Topography scale* ($L > 100$ m): The influence of these variations on dispersion phenomena can be taken into account indirectly, by defining the three-dimensional velocity field above roof level over the whole domain. This can be reconstructed by means of numerical simulations at a larger scale with prognostic models or by means of mass consistent diagnostic models assuming as an input the data collected in several stations over the whole domain. However, SIRANE currently neglects these variations and assumes an external flow developing over a flat surface with a uniformly distributed roughness (Section 5.1) due to smaller scale geometrical details. The adoption of a three-dimensional velocity field is the object of current development of the model.
- *Buildings scale* ($L \sim 10$ m): the size, spacing and orientation of the buildings has a primarily role in influencing dispersion patterns at the district scale. This information must therefore be retained in the modelled street network. Details on the procedure adopted by SIRANE to construct the street network are given below.
- *Details of the buildings geometry* ($L < 1$ m): even if the details of the buildings geometry (doors, chimneys, balconies…) can have significant influence at the local scale (Salizzoni et al., 2008; Salizzoni et al, 2009b), it is unrealistic to build complete data set including this information. For this reason small scale geometry elements are neglected by SIRANE. Nevertheless, recent studies (Salizzoni, 2006) have shown the most influent effect of the smaller scale geometry on the pollutant dispersion within the canopy can be taken into account by defining an aerodynamic roughness coefficient of the building walls and by eventually modifying the parametrisation of the mass exchange velocity between the canopy and the overlying atmospheric flow. To date SIRANE takes into account the effect of the roughness of building walls to compute the mean wind velocity along the canyon axis. Effects of small scale roughness on the pollutant transfer between canyons and the atmosphere may be taken into account in future version of the model.

Summarising, SIRANE neglects the influence of the topography and models the effects of smaller scale details of the building geometry as a uniformly distributed wall roughness. The only scale that is explicitly represented in SIRANE is therefore the building scale.

Fig. 2 shows the geometry of the buildings in a real urban district reconstructed from available geographical data sets. This geometry is still too complex to be fully represented in a dispersion model for operational purposes. A further simplification is therefore needed. The approach adopted by SIRANE is to represent a district as a network of connected streets (Fig. 1a), each of them with a rectangular section. For clarity, Fig. 3 shows an example of the simplifications of the urban geometry adopted in the model. The real urban geometry (Fig. 3a) constitutes different elements, namely the streets, courtyards and buildings, with geometries with different degrees of complexity. The flow developing within this domain is characterised by recirculating regions which retain pollutants above a fictive interface situated approximately at roof level (Fig. 3b). The region below this interface is referred to as the 'urban canopy'. Since the flow dynamics and the dispersion patterns within the canopy differ significantly from those in the atmospheric boundary layer, we split the domain into two distinct regions and adopt specific parametrisation of pollutant dispersion.

The canopy is comprised of interconnected (streets) and isolated spaces (mainly courtyards). Since emissions are rarely placed within these latter spaces, SIRANE neglects their presence, since it assumes that they do not contribute to pollutant transfer within the canopy (Fig. 3c). The concentration in these regions will be assumed equal to that in the air just above roof level in the external atmospheric flow.

The interconnected streets (Fig. 4a) are modelled as a network of boxes (Fig. 4b). Pollutant transfer between adjacent boxes and from each box to the overlying atmosphere is modelled by a series of

Fig. 2. Buildings geometry in a real urban district (Lyon, VI arrondissement).

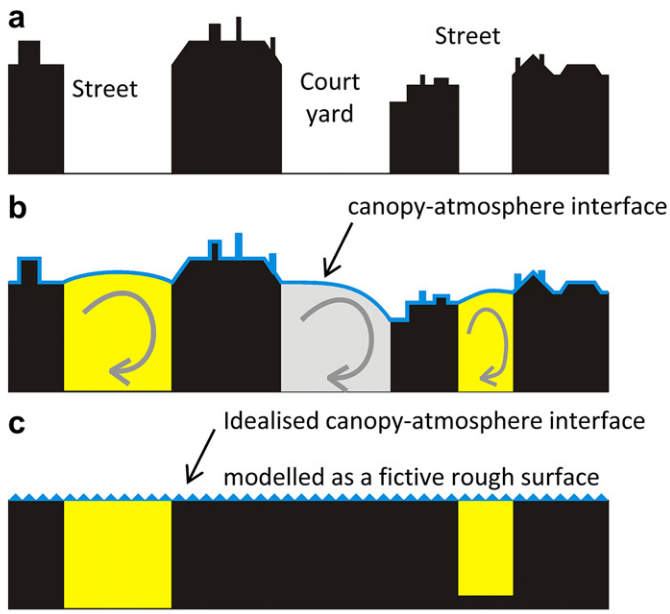

Fig. 3. Description of the urban geometry in the model SIRANE. The domain is split in two: 1) the urban canopy, represented by a street network and 2) the overlying atmospheric boundary layer flow. Regions shaded in yellow are those modelled as a street network. Regions shaded in grey are not modelled in the street network. (For interpretation of the references to colour in this figure legend, the reader is referred to the web version of this article.)

specific parametrisations whose details are elucidated in the next sections.

The external atmospheric flow is modelled as a boundary layer flow over a rough surface (blue interface in Fig. 3b) according to Monin–Obhukov theory (Section 5.1). Fig. 3c shows that in the 'canopy module' the geometry of the streets is represented explicitly (although with several simplifications), whereas in the 'external flow module' the overall effect of the canopy on the atmospheric boundary layer flow is modelled by an aerodynamic roughness length and a displacement height.

This approach is well adapted to model a district characterised by a high building density, but cannot be extended to areas with sparse density of buildings (see Fig. 4b and c). In SIRANE these regions, which may concern squares, parks or rivers are treated as open terrain and therefore modelled as part of the external atmospheric flow (cf. Fig. 4b). In particular, it is assumed that the transition between an open terrain region and the urban canopy is defined by an abrupt subjective canopy–atmosphere interface. Therefore a plume of pollutant emitted at ground level in an open terrain region will be then displaced at roof level at the canopy–atmosphere interface (blue line in Fig. 4d).

In order to differentiate the street canyons and open terrain it is necessary to adopt a threshold value for the street aspect ratio and that is not imposed in SIRANE. As a general criterion we generally assume that:

$W/H > 3 \rightarrow$ open terrain

$W/H \leq 3 \rightarrow$ street canyon

3.1. Size of the streets and traffic emissions

Summarising, SIRANE models each street as a cavity of rectangular section, characterised by its length L, width W and height H, an aerodynamic roughness parameter $z_{0,\mathrm{build}}$, with a distributed pollutant release of mass rate Q_S. The problem is therefore to estimate these quantities from urban geometry and traffic data sets, where vehicle fluxes and emissions data are stored. To this end we have developed a series of complementary computational tools, which help the user in the set up of the SIRANE network.

An example of the input data for SIRANE is given in Fig. 5a and b, showing the urban GIS data set superposed to the SIRANE network (Fig. 5a) and the traffic network (Fig. 5b). The set up of the SIRANE network is subject to many problems. The first is to estimate the uniform length, width and height of each street from the real geometry of the urban facades, which are by nature discontinuous and of variable orientation (Fig. 5a). The second is that the traffic network is often defined neglecting details of the urban geometry and therefore does not necessarily coincide with the street network (Fig. 5b). The data provided by the two networks must therefore to be merged together.

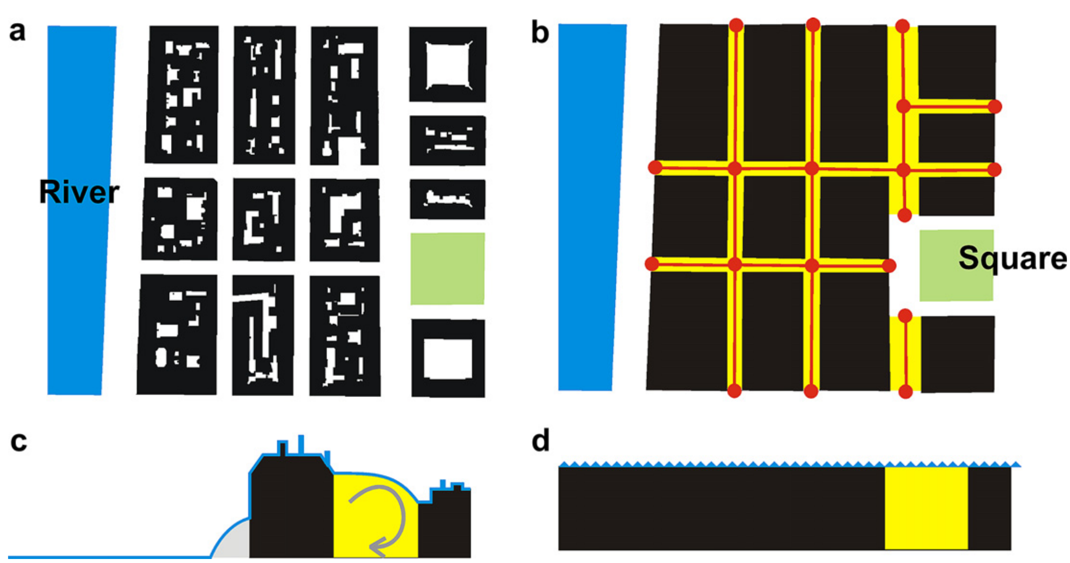

Fig. 4. Representation of a district including street canyons and open terrain zones. The regions modelled as a street network are shaded in yellow. a) Real district geometry (plan view); b) District representation in SIRANE (plan view); c) Real district geometry (cross section); d) District representation in SIRANE (cross section). (For interpretation of the references to colour in this figure legend, the reader is referred to the web version of this article.)

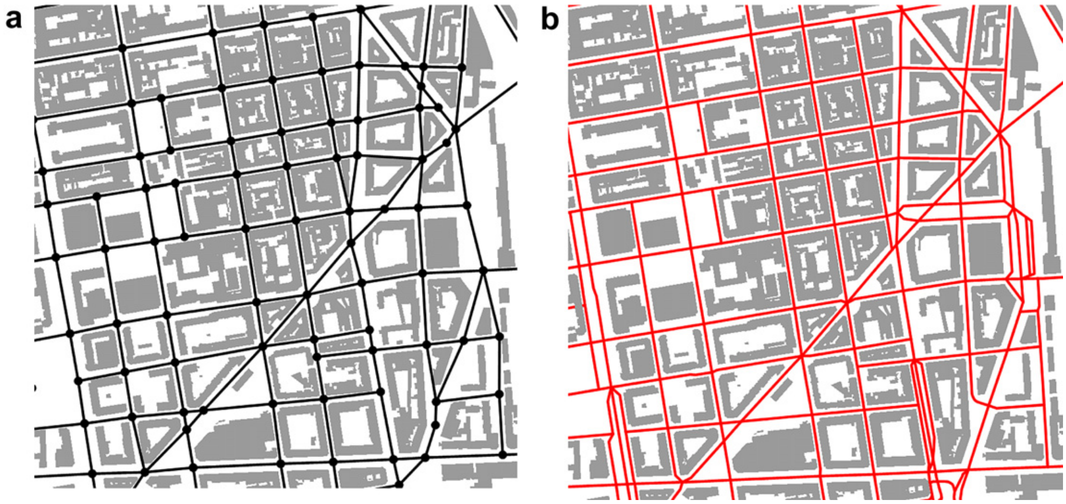

Fig. 5. Example of input data for SIRANE: a) Building geometry and SIRANE network made up of arcs (street) and nodes (intersections). b) Building geometry and traffic network.

The first step is to clearly map the SIRANE street network. This is made up by segments, which cannot cross buildings walls, and nodes, which represent street intersections (Fig. 5a). Once the network has been defined, a numerical tool computes the width, the height and the length of the street. The length is simply the distance between two nodes. The estimate of the width is more complicated and is as follows. Moving along the street axis we consider only the buildings within a buffer zone both to the right and the left sides (Fig. 6). We then retain only the building walls that have the same orientation as the street axis and which delineate the street boundary. Finally the area between these façades and the street axis (for both sides of the street) is computed and the average width of the street estimated. The same numerical tool allows us to use the GIS data set to estimate the average height of the building bordering each street segment. This numerical procedure provides also further information on the street geometry, such as the facade porosity and the facade fractioning ratio. These parameters are useful in order to evaluate if the geometry of a street is too variable to be represented by a constant value. In that case the street can be split in two or more segments joined by a fictive intersection. A result of this procedure is given in the second part of this study (Soulhac et al., submitted for publication).

The second step consists of defining a correspondence between the segments of the SIRANE street network with the segment of the traffic network (Fig. 5b). This is done with another numerical tool that projects the traffic emission values in each segment of the traffic network onto the nearest segment of the SIRANE network.

4. Flow and dispersion within the urban canopy

4.1. Flow in the urban canopy

4.1.1. Flow within the streets

The flow dynamics within a street canyon are characterised by a complex structure and this has been the object of several investigations (Dobre et al., 2005; Soulhac et al., 2008). Summarising, this flow is made up of a recirculating component on the cross section of the street which is superposed on a flow along the street

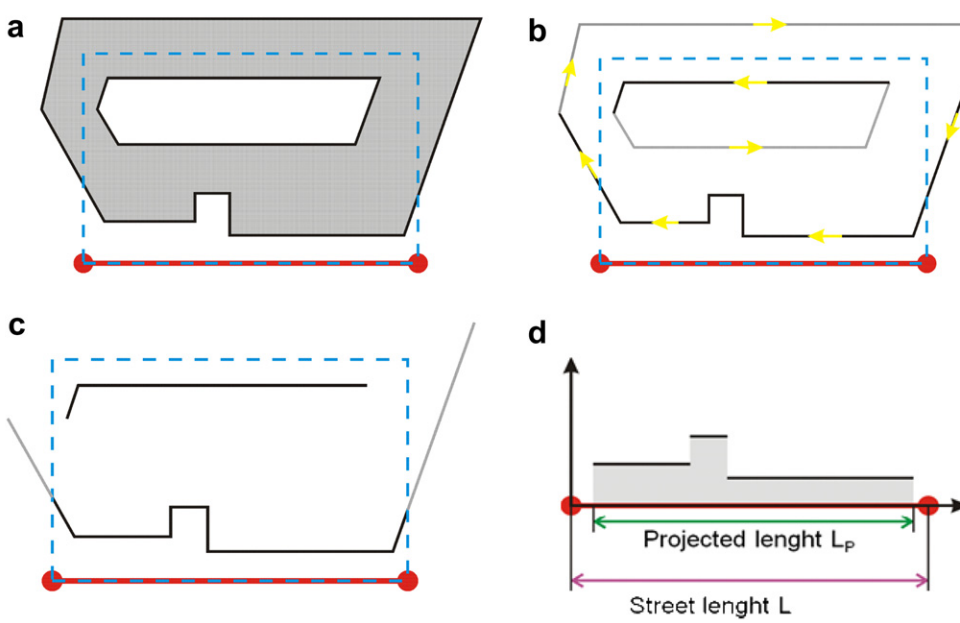

Fig. 6. Procedure for the estimate of the street widths in the SIRANE network.

axis (Soulhac et al., 2008). The dynamics of this flow depend on the geometrical details of the streets and on the dynamics of the external boundary layer flow, which determines the forcing of the flow within the street. Since SIRANE has been conceived to compute spatially averaged concentrations within each street, we are not interested in the details of the flow within it. Instead we concentrate on the spatially averaged wind velocity along the street axis, U_{street}, which is responsible for a mean advective flux at the upstream and downstream edges of the canyon.

The averaged velocity U_{street} is assumed to be given by a balance between the turbulent entrainment at roof level and the drag on building walls (Soulhac et al., 2008). We therefore neglect both the effect of pressure gradients and the other entrainment effects of moving vehicles (e.g. Vachon et al., 2002). Applying these assumptions Soulhac et al. (2008) show that the velocity U_{street} can be computed as:

$$U_{\text{street}} = U_H \cos(\varphi)\frac{\delta_i^2}{HW}\left[\frac{2\sqrt{2}}{C}(1-\beta)\left(1-\frac{C^2}{3}+\frac{C^4}{45}\right)+\beta\frac{2\alpha-3}{\alpha} + \left(\frac{W}{\delta_i}-2\right)\frac{\alpha-1}{\alpha}\right]$$

$$\text{with}\begin{cases}\alpha = \ln\left(\dfrac{\delta_i}{z_{0,\text{build}}}\right)\\ \beta = \exp\left[\dfrac{C}{\sqrt{2}}\left(1-\dfrac{H}{\delta_i}\right)\right]\\ U_H = u_*\sqrt{\dfrac{\pi}{\sqrt{2}\kappa^2 C}\left[Y_0(C)-\dfrac{J_0(C)Y_1(C)}{J_1(C)}\right]}\\ C \text{ solution of } \dfrac{z_{0,\text{build}}}{\delta_i} = \dfrac{2}{C}\exp\left[\dfrac{\pi}{2}\dfrac{Y_1(C)}{J_1(C)}-\gamma\right]\\ \delta_i = \min(H;W/2)\end{cases} \quad (1)$$

where J_0, J_1, Y_0 and Y_1 are Bessel functions, u_* is the friction velocity of the overlying boundary layer flow, φ is the external wind direction with respect to the street axis, H and W are the street height and width, respectively, and $z_{0,\text{build}}$ is the aerodynamic roughness of canyon walls. The averaged velocity U_{street} is used in order to compute the mass balance within each street and the balance of air fluxes at intersections (Section 4.2.1). For further details on the model of the flow within the street we refer the reader to Soulhac et al. (2008).

4.1.2. Flow within street intersections

The flow patterns within a street intersection are strongly related to the size, orientation and relative distance of the buildings bordering the streets that form the intersection (Soulhac et al., 2009). In this study the authors identify two kinds of intersections. When the street ratio of the streets is sufficiently high, forming a 'simple intersection', the flow within the intersection is almost decoupled from that in the external flow. Conversely, for low aspect ratios, in 'large squares', the external flow penetrates deeply into the urban canopy. In the present version of SIRANE the pollutant dispersion in large squares is modelled identically to that in open terrain whereas the pollutant dispersion in simple intersections is modelled by a specific parametric module (Section 5.2.2). In order to distinguish these two cases a threshold value for the street aspect ratio is need. In our previous work we have so far considered an intersection to be 'simple' if its diameter $W < 3H$. Conversely, if $W > 3H$, the intersection is designated an 'open terrain region' (Soulhac et al., submitted for publication).

The aim of the flow model within street intersections is to determine how the air fluxes are split between the different streets connected at the intersection. Numerical simulations (Soulhac et al., 2009) have shown that the flow in a street intersection can be modelled by taking into account two main features: the horizontal air flux from one street to another and the vertical air flux between the urban canopy and the external atmosphere.

The horizontal air flux is estimated assuming that the flow dynamics within the intersection is two-dimensional, i.e. that the topology of the streamlines does not depend on the vertical distance from the ground (Soulhac et al., 2009). This assumption is mainly based on the observation that the streamlines hardly cross each other (Fig. 7a) and there is therefore very little vertical variation in the mean flow at any point in the intersection.

The vertical air flux is modelled by a simple balance of the air volumes entering and leaving the intersection. When the air flow rate through the cross sections of the upwind and downwind streets are different, a vertical air flux results. The simplest example is given for a junction of two streets with varying cross section as shown in Fig. 7b. To model the behaviour of these flow patterns, SIRANE adopts a drastic simplification of the flow dynamics. Firstly it is assumed that the mean velocity within each street connected to the intersection verifies equation (1). The air flux in each street of index i, connected to the intersection, is computed as:

$$P_{\text{street},i} = \xi HWU_{\text{street},i} \quad (2)$$

where $\xi = 1$ for streets upwind of the intersections (entering flux) and $\xi = -1$ for downwind streets. The vertical air flux leaving the intersection can then be computed by applying mass conservation over the volume of the intersection:

$$P_{\text{vert}} = \sum_{i \in \text{intersection}} P_{\text{street},i} \quad (3)$$

To estimate the flux of pollutant from one street to another it is necessary to compute the convective flux $P_{i,j}$ between the streets i and j of an intersection. To that end, it is assumed that the streamlines from different street upwind of the intersection do not cross and that the flow within the intersection is two-dimensional (Fig. 8). The coefficient $P_{i,j}$ is then determined by simply estimating the mean air fluxes entering and leaving the intersection.

4.2. Dispersion within the canopy

Since the pollutant concentration within a street canyon depends on that in the surrounding streets and the overlying atmosphere, we cannot compute this concentration aside from that in the other canyons. It is thus necessary to solve a system of linear equations with unknown the spatially averaged concentration in each street of the computational domain. In the following paragraph we present the equations composing this system.

4.2.1. Spatially averaged concentration within street canyons

The (time hourly) spatially averaged concentration C_{street} in each street of the district is modelled by a box model, computing

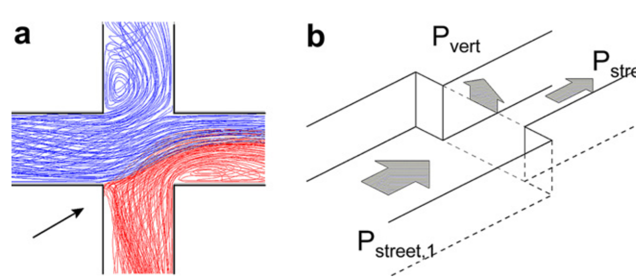

Fig. 7. Sketch of the flow patterns within street intersections (Soulhac et al., 2009). a) Horizontal sections of the streamlines – numerical simulations (Soulhac et al., 2009) b) Vertical air flux at the junction of two streets with different widths ($|P_{\text{street},1}| > |P_{\text{street},2}|$).

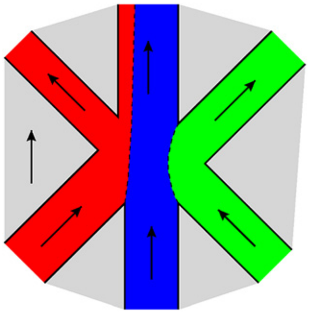

Fig. 8. Model of the air fluxes on the horizontal plane within a street intersection.

a balance of the pollutant fluxes entering and leaving the street volume (Fig. 9). Assuming steady state conditions, this mass balance over the street volume can be written as:

$$\underbrace{Q_S + Q_I + Q_{\text{part},H}}_{\text{Fluxes in}} = \underbrace{Q_{H,\text{turb}} + HWU_{\text{street}}C_{\text{street}} + Q_{\text{part,gr}} + Q_{\text{wash}}}_{\text{Fluxes out}} \tag{4}$$

where Q_S is the pollutant mass rate emitted within the street, Q_I represents the flux of pollutants advected by the mean flow along the street axis and entering at the upwind intersection (Section 4.2.3), $Q_{\text{part},H}$ is the sedimentation flux of solid particles entering the street through the street-atmosphere interface, $HWU_{\text{street}}C_{\text{street}}$ is the flux of pollutants advected by the mean flow along the street axis and leaving at the downstream edge of the street, $Q_{H,\text{turb}}$ is the flux of pollutants exchanged by turbulent diffusion at the street-atmosphere interface (Section 4.2.2), $Q_{\text{part,gr}}$ is the deposition flux of solid particles towards the ground (any eventual re-suspension is taken into account by the source term Q_S) and Q_{wash} is the amount of pollutant per unit time washed-out by wet deposition (Section 6.2)

Equation (4) allows us to relate the spatially averaged pollutant concentration within the street to that in the upwind streets and to that above roof level, in the external atmospheric flow.

In the following paragraphs we present the parametric relations adopted to model all terms of (4). For brevity we will not give details on the model for $Q_{\text{part},H}$ since dry deposition phenomena will be neglected in the model validation presented in the second part of this study (Soulhac et al., submitted for publication).

4.2.2. Turbulent transfer street-atmosphere

The turbulent transfer between a street canyon and the overlying atmospheric flow is an unsteady process characterised by high intermittency. The energy for this process is provided by the kinetic energy of the external flow, whose forcing action on the canyon flow is determined by the dynamics of a region of high shear at the interface between the two parts of the flow. The unstable condition of this region results in a flapping motion of the shear layer and a subsequent intermittent inflow of turbulent structures into the canyon which induces a bulk transfer between the canyon and the external flow (Salizzoni et al., 2009a).

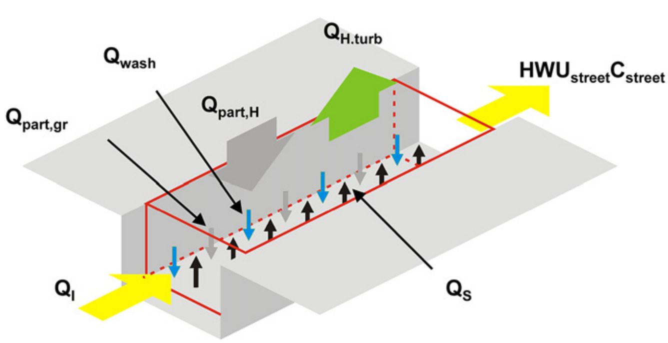

Fig. 9. Mass balance within a street canyon.

Using the box model approach, we can parameterise this turbulent transfer by means of an exchange velocity, referred to as u_d. The velocity u_d represents an integral variable, which therefore depends on all features characterising the turbulent flow within the street canyon. Generally, we can assume that u_d depends on the geometrical parameters of the canyon, the dynamical conditions of the atmospheric turbulence and the wind direction.

Several studies have attempted to define the dependence of u_d on the dynamical conditions of the external flow (Kim and Baik, 2003; Salizzoni et al., 2009a), the wind direction (Soulhac, 2000) and the canyon geometry (Hoydysh and Dabberdt, 1988; Salizzoni, 2006). More recently some authors have also investigated the influence of thermal fluxes at canyon walls (Sini et al., 1996; Offerle et al., 2007) and trees within the canyon (Buccolieri et al., 2009).

These studies have shown that the exchange velocity is driven by the external flow velocity U_{ext} but depends also on the turbulence level and the structure of the atmospheric flow (Salizzoni et al., 2009a). Concerning the canyon geometry, it is well know that u_d is strongly dependent upon the aspect ratio of the street (Hoydysh and Dabberdt, 1988), the form of the canyon (Soulhac, 2000), its length and the orientation of the external wind. However, more recent studies have demonstrated that even smaller scale geometrical details can significantly alter the vertical mass exchange (Salizzoni, 2006).

It is worth noting that the mechanisms governing these transport processes are extremely complex and that any analytical model of this mass transfer requires simplifying assumptions.

As a first approximation, SIRANE assumes that u_d does not depend on the geometry of the canyon and is therefore only defined by the external flow condition. The transfer velocity can be considered proportional to σ_w, the intensity of the standard deviation of the vertical velocity at roof level, and estimated (Soulhac, 2000; Salizzoni et al., 2009a) as

$$u_d = \frac{\sigma_w}{\sqrt{2\pi}} \tag{5}$$

Therefore the vertical flux $Q_{H,\text{turb}}$ in (4) can be expressed as:

$$Q_{H,\text{turb}} = \frac{\sigma_w WL}{\sqrt{2\pi}}\left(C_{\text{street}} - C_{\text{street,ext}}\right) \tag{6}$$

where C_{street} and $C_{\text{street,ext}}$ are the mean concentration within and above the street, respectively, W and L are the street length and width and σ_w is the standard deviation of the vertical velocity computed at roof level as indicated in Section 5.1.3.

4.2.3. Pollutant transfer at street intersections

The aim of the pollutant transfer model at street intersections is to estimate the upwind pollutant flux $Q_{I,j}$ entering street j. The rate of pollutant transfer between two crossing streets i and j is a function of the exchange coefficient $P_{i,j}$, which in turn depends on the wind direction φ. However, this coefficient does not take into account the turbulent mixing but only the topology of the mean streamlines within the intersections (Soulhac et al., 2009). By assuming that the turbulent mixing within the intersection mainly depends on larger scale fluctuations, its effect can be modelled by considering the standard deviation of the wind direction. We can therefore define a time averaged exchange coefficient as:

$$\hat{P}_{i,j}(\varphi_0) = \int f(\varphi-\varphi_0)\,P_{i,j}(\varphi)\,\mathrm{d}\varphi \tag{7}$$

$$\text{with } f(\varphi-\varphi_0) = \frac{1}{\sigma_\varphi\sqrt{2\pi}}\exp\left[-\frac{1}{2}\left(\frac{\varphi-\varphi_0}{\sigma_\varphi}\right)^2\right]$$

where φ_0 is the average wind direction and σ_φ the standard deviation of the wind direction.

The flux leaving the intersection from street j can be expressed by taking into account the contribution of all streets connected at the intersection:

$$Q_{I,j} = \sum_i \hat{P}_{i,j}(\varphi_0)C_{\text{street},i} + P_{\text{ext}\to j}C_{I,\text{ext}} \tag{8}$$

The second term of (7) represents the flux from the external flow (therefore related to a concentration $C_{I,\text{ext}}$) and which enters the intersection vertically. The flux $P_{\text{ext}\to j}$ is computed considering only the case of air from the external flow entering the intersection ($P_{\text{vert}} < 0$) and assuming that the incoming flux is distributed in the streets downwind of the intersection proportionally to the flow rate in each street:

$$P_{\text{ext}\to j} = \max(-P_{\text{vert}};0)\frac{P_{\text{street},j}}{\sum\limits_{\text{street downwind to the intersection}} P_{\text{street},i}} \tag{9}$$

5. Flow and dispersion above the roof level

5.1. Flow

The description of the atmospheric boundary layer flow in SIRANE has three main objectives:

- To determine the characteristics of the atmospheric flow and turbulence needed to estimate the pollutant dispersion in the external atmospheric flow (Section 5.2).
- To compute the parameters describing the flow within the canopy as a function of the forcing induced by the external atmospheric flow (Section 4.1).
- To evaluate the intensity of the atmospheric turbulence in the lower part of the boundary layer flow in order to estimate the turbulent pollutant fluxes between the urban canopy and the overlying atmosphere (Section 4.2.2).

The external boundary layer flow is modelled using Monin–Obukhov similarity theory. The flow is assumed homogeneous in the horizontal plane. Therefore all dynamical parameters of the flow are assumed to depend on the vertical coordinate z only. It is well known that in the flow above roughness elements this condition is not valid below a height (Fig. 10) which is approximately equal to $z_* = H + 1.5\,W$ (Raupach et al., 1980). For $z < z_*$, the flow is directly influenced by the wake of each building and the flow cannot be considered to be horizontally homogeneous. Nevertheless, the dynamical properties of this region of the flow, usually referred to as the 'roughness sub-layer', cannot be represented satisfactorily by a universal description, since it depends on the particularity of each

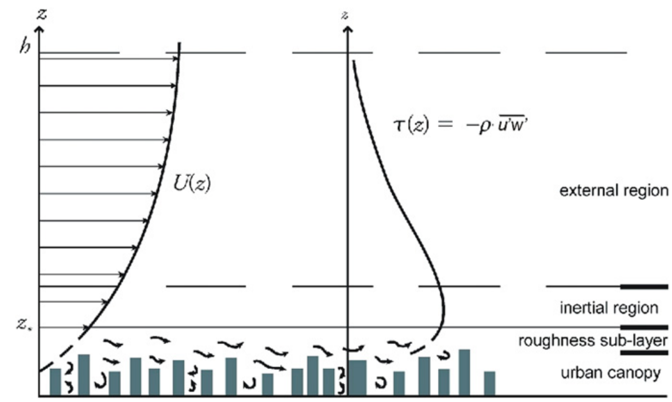

Fig. 10. Vertical structure of the urban boundary layer in neutral conditions.

single building geometry (Raupach et al., 1980). Therefore, for simplicity, SIRANE neglects the presence of the roughness sub-layer and assumes that the profiles given by the Monin–Obukhov theory extend through the whole boundary layer down to roof level.

The external boundary layer flow model presented in the following paragraphs is mainly inspired by reviews of meteorological pre-processor given by Holtslag and Van Ulden (1983), Fisher et al. (1998) and of the parametrisations adopted by the ADMS model (CERC, 2001).

5.1.1. Mean velocity and temperature profiles

According to Monin–Obukhov similarity theory, the mean velocity field within the atmospheric boundary layer above roof level may be modelled by the following relation (Garratt, 1992):

$$u(z) = \frac{u_*}{\kappa}\left[\ln\left(\frac{z-d_{\text{district}}+z_{0,\text{district}}}{z_{0,\text{district}}}\right) - \left(\psi_m\left(\frac{z-d_{\text{district}}+z_{0,\text{district}}}{L_{\text{MO}}}\right)-\psi_m\left(\frac{z_{0,\text{district}}}{L_{\text{MO}}}\right)\right)\right] \tag{10}$$

where $z_{0,\text{district}}$ and d_{district} are the aerodynamic roughness and the displacement height of the district (Section 5.1.2) and L_{MO} is the Monin–Obukhov length, defined as

$$L_{\text{MO}} = -\frac{\rho c_p \theta u_*^3}{\kappa g H_0}$$

being H_0 the sensible heat flux between the ground and the atmosphere (see Appendix). The function, ψ_m is defined as (Businger et al., 1971):

$$\begin{cases} \psi_m(\zeta) = 2\ln[(1+x)/2] + \ln[(1+x^2)/2] - 2\arctan(x) + \pi/2 \quad \text{if } L_{\text{MO}} < 0 \quad \text{(unstable)} \\ \text{with } x = (1-16\zeta)^{1/4} \\ \psi_m(\zeta) = 0 \quad \text{if } L_{\text{MO}} = 0 \quad \text{(neutral)} \\ \psi_m(\zeta) = -5\zeta \quad \text{if } L_{\text{MO}} > 0 \quad \text{(stable)} \end{cases} \tag{11}$$

The vertical profile of potential temperature is given by Garratt (1992):

$$\theta(z) = \theta_0 + \frac{\theta_*}{\kappa}\left[\ln\left(\frac{z+z_T}{z_T}\right) - \left(\psi_h\left(\frac{z+z_T}{L_{\text{MO}}}\right)-\psi_h\left(\frac{z_T}{L_{\text{MO}}}\right)\right)\right] \tag{12}$$

where θ_0 is the potential temperature at ground level and z_T is the thermal roughness of the district (Section 5.1.2) and the function ψ_h is defined as:

$$\begin{cases}\psi_h(\zeta) = 2\ln[(1+x)/2] & \text{if } L_{MO} < 0 \quad \text{(unstable)} \\ \text{with } x = \sqrt{1-16\zeta} & \\ \psi_h(\zeta) = 0 & \text{if } L_{MO} = 0 \quad \text{(neutral)} \\ \psi_h(\zeta) = -5\zeta & \text{if } L_{MO} > 0 \quad \text{(stable)}\end{cases} \tag{13}$$

5.1.2. Aerodynamic roughness, displacement height and thermal roughness

The influence of the buildings composing the urban district on the vertical profiles of mean velocity is modelled, as it is usual, by two parameters, the aerodynamic roughness length $z_{0,\text{district}}$ and the displacement height d_{district}. Both of them are input parameters of SIRANE, and have therefore to be previously computed by the user. These quantities can be estimated with several empirical models, which are based on site observations and wind tunnel experiments. An extensive review of these models is given by Grimmond and Oke (1999) whereas an example of a procedure of their estimate a real case study is presented in the second part of this study (Soulhac et al., submitted for publication).

The thermal roughness is computed from the aerodynamic roughness by the following relation (Garratt, 1992):

$$z_T = z_0 \exp\left[-\kappa\left(6.2\text{Re}_s^{1/4} - 5\right)\right] \quad \text{with } \text{Re}_s = \frac{u_* z_0}{\nu_a} \tag{14}$$

5.1.3. Atmospheric turbulence

The intensity of the turbulent fluctuations within the atmospheric boundary layer can be characterised by vertical profiles of the standard deviation of the three components of the wind velocity σ_u, σ_v and σ_w. The profiles adopted in SIRANE are those given by the following relations (Hunt et al., 1988; CERC, 2001):

Standard deviation σ_v

$$\begin{cases}\sigma_v = \sqrt{0.3\, w_*^2 + [2\, u_*\,(1-0.8\, z/h)]^2} & \text{if } L_{MO} < 0 \text{ - unstable} \\ \sigma_v = 2\, u_*\,(1-0.8\, z/h) & \text{if } L_{MO} \to \infty \text{ - neutral} \\ \sigma_v = 2\, u_* (1-0.5\, z/h)^{3/4} & \text{if } L_{MO} > 0 \text{ - stable}\end{cases} \tag{15}$$

Standard deviation σ_w

$$\begin{cases}\sigma_w = \sqrt{\sigma_{wc}^2 + \sigma_{wn}^2} & \text{if } L_{MO} < 0 \text{ - unstable} \\ \text{with } \sigma_{wc} = \sqrt{0.4}\, w_*\, 2.1 (z/h)^{1/3} (1-0.8z/h) \text{ and } \sigma_{wc} = 1.3u_*(1-0.8z/h) & \\ \sigma_w = 1.3u_*(1-0.8z/h) & \text{if } L_{MO} \to \infty \text{ -neutral} \\ \sigma_w = 1.3u_*(1-0.5z/h)^{3/4} & \text{if } L_{MO} > 0 \text{ -stable}\end{cases} \tag{16}$$

where h is the boundary layer height (Section 5.1.4) and w_* is the convective velocity scale, defined as:

$$w_* = u_*\left(\frac{h}{\kappa L_{MO}}\right)^{1/3} \tag{17}$$

The Lagrangian integral time scale is modelled as (Hunt et al., 1988; CERC, 2001):

$$\begin{cases}T_L = \dfrac{1}{1.3\sigma_w}\left[\dfrac{2.5}{z+z_{0,\text{district}}} + \dfrac{N}{\sigma_w} + \dfrac{4}{h} + \dfrac{1}{z_u}\right]^{-1} & \text{stable atmosphere} \\ T_L = \dfrac{\dfrac{\dfrac{h}{L_{MO}} + \dfrac{1}{3}}{\dfrac{h}{L_{MO}} + 1}\left[\dfrac{0.6}{z+z_{0,\text{district}}} + \dfrac{\partial u}{\partial z} + \dfrac{2}{h} + \dfrac{1}{z_u}\right]}{\sigma_w} & \text{unstable atmosphere} \\ \text{with } z_u = \max\left(h - z; \dfrac{\sigma_w}{N}\right) & \end{cases} \tag{18}$$

where $N = \sqrt{\frac{g}{T_0}\frac{\partial \theta}{\partial z}}$ is the Brunt–Väisälä frequency and T_0 is the temperature at ground level.

5.1.4. Boundary layer height

The height h of the atmospheric boundary layer is strictly related to its thermal stratification. In a stable or neutral atmosphere, h can be considered as time independent and can therefore be computed as a function of the meteorological condition at a given time. In an unstably stratified atm h varies with time because of a thermal forcing induced by the thermal fluxes from the ground (Batchvarova and Gryning, 1991). The boundary layer depth in unstable conditions depends then not only on the conditions at a given time but also on the conditions at previous times. The relations adopted to model the boundary layer depths in different stability conditions are:

Stable atmosphere ($L_{MO} > 0$) (Nieuwstadt and Tennekes, 1981)

$$h = \frac{L_{MO}}{3.8}\left(-1 + \sqrt{1 + 2.28\frac{u_*}{fL_{MO}}}\right) \tag{19}$$

Neutral atmosphere ($L_{MO} \to \infty$)

In a neutrally stratified atmosphere (19) reduces to:

$$h = 0.3\frac{u_*}{f} \tag{20}$$

Unstable atmosphere ($L_{MO} < 0$) Batchvarova and Gryning (1991)

$$\frac{\mathrm{d}h}{\mathrm{d}t} = \frac{1.4w_*^3 + 5u_*^3}{\frac{g}{T_0}\gamma_\theta^{\text{ext}} h^2} \tag{21}$$

where $\gamma_\theta^{\text{ext}} = \partial\theta/\partial z$ is the vertical gradient of potential temperature in the atmosphere and T_0 is the temperature at ground level. Assuming that these parameters are time independent, this differential equation has the implicit analytical solution

$$t_2 - t_1 = \frac{\chi^2}{2a_1}\left[\left(\frac{h_2}{\chi} - 1\right)^2 - \left(\frac{h_1}{\chi} - 1\right)^2 + 2\ln\left(\frac{h_2 + \chi}{h_1 + \chi}\right)\right],$$
$$\text{with}\begin{cases}\chi = \dfrac{a_2}{a_1} \\ a_1 = \dfrac{1.4H_0}{\rho_a C_p \gamma_\theta^{\text{ext}}} \text{ and } a_2 = \dfrac{5u_*^3 T_0}{g\gamma_\theta^{\text{ext}}}\end{cases} \tag{22}$$

Here, h_1 and h_2 are the boundary layer depths at time t_1 and t_2, respectively. This relation is used to compute the boundary layer depth for each hourly time step. The computation is initialised at the sunrise with the nocturnal value given by equation (19).

5.2. Dispersion over roof level

5.2.1. Gaussian plume model

The pollutants transported in the urban atmospheric boundary layer are emitted by elevated sources (stacks) or within the urban canopy. These latter sources, whose intensity is referred to as $Q_{H,\text{turb}}$ in equation (4), are modelled as a series of point sources at roof level (Fig. 11). $Q_{H,\text{turb}}$ can therefore be positive when the pollutant flux is directed from the streets to the atmosphere, or negative, if the flux is directed downward from the atmosphere to the underlying street canyons. In SIRANE, line source of pollutant in open terrain are modelled as a series of point sources.

The pollutant dispersion phenomena taking place above roof level are simulated by a Gaussian plume model. Plume reflections at the top of the boundary layer and at roof level $z = H_{\text{build}}$ (H_{build} represents the mean height of the buildings over the district) are simulated by the image source technique (Fig. 12).

Therefore, the concentration field resulting from a point source of pollutant placed at (x_s, y_s) is given by :

$$c(x,y,z) = \frac{Q_{S,\text{eff}}}{\sqrt{2\pi}U_m\sigma_y}\exp\left[-\frac{1}{2}\frac{(y-y_s)^2}{\sigma_y^2}\right] \times \left[\text{pdfz}\left(z-H_{s,\text{eff}}\right) + \text{pdfz}\left(z-2H_{\text{build}}+H_{s,\text{eff}}\right) + \text{pdfz}\left(z-2h+H_{s,\text{eff}}\right)\right] \quad (23)$$

where $Q_{S,\text{eff}}$ is the effective mass flux emitted by the source (taking into account the effects of wet deposition, Section 6.2), σ_y is the standard deviation of the plume in the transverse direction (Section 5.1.4) and $H_{s,\text{eff}}$ is the effective height of the source, computed as the sum of the real source height H_s and the plume rise ΔH, estimated according the model of Briggs (1984).

U_m is the plume advective velocity defined:

$$U_m = \frac{\int u(z)\cdot c(x,y,z)\text{d}z}{\int c(x,y,z)\text{d}z} \quad (24)$$

The function pdfz represents the vertical distribution of concentrations. In a neutral or stable boundary layer, this distribution has a Gaussian form:

$$\text{pdfz}(z) = \frac{1}{\sqrt{2\pi}\sigma_z}\exp\left[-\frac{1}{2}\frac{z^2}{\sigma_z^2}\right] \quad (25)$$

where σ_z is the vertical standard deviation of the plume (Section 4.2.2). In an unstable atmosphere, the convective upward thermals

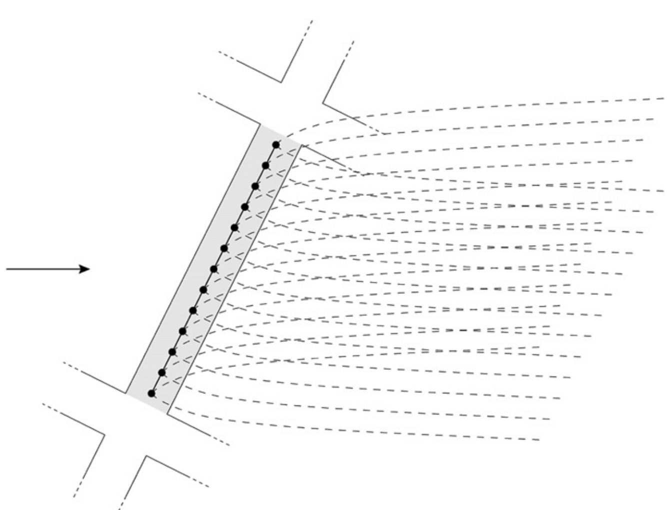

Fig. 11. Modelling of pollutant transfer at roof level as a series of point sources; the arrow indicates the wind direction.

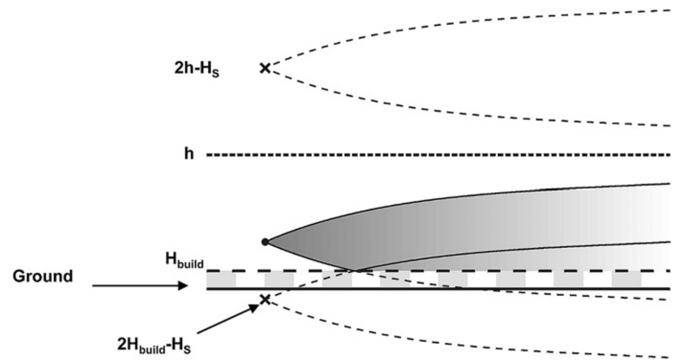

Fig. 12. Plume reflection at the top of the urban canopy and at the boundary layer.

induce an asymmetric distribution of the mean concentration (Luhar and Britter, 1989). This effect can be modelled with a bi-Gaussian distribution:

$$\text{pdfz}(z) = \frac{a_+H(z-\hat{w}t)}{\sqrt{2\pi}\sigma_{z+}}\exp\left[-\frac{1}{2}\frac{(z-\hat{w}t)^2}{\sigma_{z+}^2}\right] + \frac{a_-[1-H(z-\hat{w}t)]}{\sqrt{2\pi}\sigma_{z-}}\exp\left[-\frac{1}{2}\frac{(z-\hat{w}t)^2}{\sigma_{z-}^2}\right]$$

$$\text{with} \begin{cases} \hat{w} = -\dfrac{\sigma_{wc}}{2} \\ \sigma_{z+} = \dfrac{\sigma_{w+}t}{\sqrt{1+t/2T_L}} \text{ and } \sigma_{z-} = \dfrac{\sigma_{w-}t}{\sqrt{1+t/2T_L}} \\ \sigma_{w+} = \dfrac{\sigma_w}{k} + \sqrt{\dfrac{\pi}{32}}\sigma_{wc} \text{ and } \sigma_{w-} = \dfrac{\sigma_w}{k} - \sqrt{\dfrac{\pi}{32}}\sigma_{wc} \\ a_+ = k\dfrac{\sigma_{w+}}{\sigma_w} \text{ and } a_- = k\dfrac{\sigma_{w-}}{\sigma_w} \\ k = \left[1+\left(\dfrac{1}{4}-\dfrac{3\pi}{32}\right)\left(\dfrac{\sigma_{wc}}{\sigma_w}\right)^2\right]^{-1/2} \end{cases} \quad (26)$$

where σ_{wc} is the convective component of the vertical velocity fluctuation (Section 5.1.3). The Gaussian model is a function of parameters which depend on the vertical coordinate z. This distance from the ground is computed as an average height, referred to as z_m, where

$$z_m = \frac{\int z\cdot c(x,y,z)\text{d}z}{\int c(x,y,z)\text{d}z} \quad (27)$$

and $c(x,y,z)$ is the pollutant distribution within the plume.

5.2.2. Modelling of plume standard deviations

The standard deviations σ_y and σ_z in the relations (25) and (26) are functions of the downstream distance from the source x. Their spatial evolution essentially depends on the intensity of atmospheric turbulence and consequently on the thermal stratification of the atmosphere. SIRANE assumes two kinds of parametrisation of these terms. The first is based on the well known Pasquill–Gifford stability classes (Briggs, 1973; Pasquill and Smith, 1983). The second is based on a continuous parametrisation of these standard deviations, based on the approaches proposed by Weil (1985), Venkatram (1992) and CERC (2001):

Standard deviation σ_y

$$\sigma_y = \sqrt{\sigma_{y,s}^2 + \left(\sigma_\varphi \frac{\pi}{180} x\right)^2}$$
$$\text{with} \begin{cases} \sigma_{y,s} = \sqrt{\sigma_{y,c}^2 + \sigma_{y,n}^2} \text{ with } \begin{cases} \sigma_{y,c} = \sqrt{0.3}\dfrac{w_* t}{\sqrt{1 + 0.75^{1/3}\dfrac{w_* t}{h}}} \\ \sigma_{y,n} = 2\left(1 - 0.8\dfrac{z}{h}\right) \dfrac{u_* t}{\sqrt{1 + 2.5\dfrac{u_* t}{h}}} \end{cases} & \text{if } L_{MO} < 0\text{-unstable} \\ \sigma_{y,s} = \dfrac{\sigma_v t}{\sqrt{1 + 2.5\dfrac{u_* t}{h}}} & \text{if } L_{MO} \to \infty \text{ -neutral} \\ \sigma_{y,s} = \dfrac{\sigma_v t}{\sqrt{1 + 2.5\dfrac{u_* t L_{MO}}{h^2}}} & \text{if } L_{MO} > 0 \text{ -stable} \end{cases} \quad (28)$$

Standard deviation σ_z

$$\begin{cases} \sigma_z = \dfrac{\sigma_w t}{\sqrt{1 + \dfrac{t}{2T_L}}} & \text{if } L_{MO} < 0 \text{ -unstable} \\ \sigma_z = 0.4\sigma_w t & \text{if } L_{MO} \to \infty \text{ -neutral} \\ \sigma_z = \dfrac{\sigma_w t}{\sqrt{6.25 + \dfrac{N^2 t^2}{1 + 2Nt}}} & \text{if } L_{MO} > 0 \text{ -stable} \end{cases} \quad (29)$$

where σ_v, σ_w, σ_φ and N are computed at the averaged height of the plume z_m.

6. Physico-chemical processes

We briefly present here the model of the physico-chemical transformation included in SIRANE. These concern the Chapman cycle for nitrogen oxides and ozone transformations and wet deposition. SIRANE also includes a model for dry deposition flux, referred to as $Q_{part,H}$ (4), that is not presented here.

6.1. Chemical reactions

Pollutant dispersion phenomena at the district scale are characterised by a typical time scale of a few tens of minutes. Most chemical transformations occurring in the atmosphere have longer time scales and can therefore be neglected here. Nevertheless some chemical reactions take place over periods which are sufficiently short so as to modify significantly the concentration field of some pollutant species. This happens for example for nitrogen oxides whose reactions induce the formation or the destruction of ozone (Seinfeld, 1986). For this reason SIRANE adopts a simple chemical model to take into account these transformations. The nitrogen cycle in the atmosphere involves several complex reactions. However the main chemical transformations are taken into account by the Chapman cycle:

$$\begin{cases} NO_2 + h\nu \xrightarrow{k_1} NO + O^\bullet \\ O^\bullet + O_2 \xrightarrow{k_2} O_3 \\ NO + O_3 \xrightarrow{k_3} NO_2 + O_2 \end{cases} \quad (30)$$

where k_1, k_2 and k_3 are kinetic constant of reaction. It is worth mentioning that the reactivity of the radical $O^\bullet$ is high, so that the characteristic time of the reaction is negligible compared to that of the other reactions. Firstly, SIRANE computes the concentration field of nitrogen dioxides NO_x ($NO + NO_2$) as if it were a passive pollutant. Secondly, by assuming a photo-stationary equilibrium condition, the chemical model implemented in SIRANE provides the estimate of the concentration of NO, NO_2 and O_3 from the concentration of NO_x:

$$\begin{cases} [NO_2] = \dfrac{b - \sqrt{b^2 - 4c}}{2} \\ [NO] = [NO]_b + [NO_2]_b + [NO_x]_d - [NO_2] \\ [O_3] = [O_3]_b + [NO_2]_b + \zeta[NO_x]_d - [NO_2] \\ b = \dfrac{k_1}{k_3} + [O_3]_b + [NO]_b + 2[NO_2]_b + (1 + \zeta)[NO_x]_d \\ c = \left([O_3]_b + [NO_2]_b + \zeta[NO_x]_d\right)\left([NO]_b + [NO_2]_b + [NO_x]_d\right) \end{cases} \quad (31)$$

Here, the quantities within square brackets represent molar concentrations, $[NO_x]_d$ is the concentration of the passive quantity NO_x computed by SIRANE, $[NO]_b$, $[NO_2]_b$ and $[O_3]_b$ are the background concentrations of NO, NO_2 and O_3 respectively, and ζ is the ratio $[NO_2]/[NO_x]$ at the emission.

In order to solve the systems of equation two options are possible. The first is to assume that the ratio k_1/k_3 is constant with time and uniform in the whole district. In this case the value of the ratio k_1/k_3 can be fixed by the user as an input parameter. The second is consider to that ratio k_1/k_3 is uniform over the domain but is not constant for each time step. In fact, k_1 (NO_2 photolysis rate) depends on the solar light intensity whereas k_3 depends on the temperature. These dependences can be modelled by the relations (Kasten and Czeplak, 1980; Seinfeld, 1986)

$$\begin{cases} k_1 = \dfrac{1}{60}\left(0.5699 - \left[9.056 \cdot 10^{-3}(90 - \chi)\right]^{2.546}\right)\left(1 - 0.75\left[\dfrac{Cld}{8}\right]^{3.4}\right)\left[s^{-1}\right] \\ k_3 = 1.325 \cdot 10^5 \exp\left(-\dfrac{1430}{T}\right)\left[m^3 \text{ mole}^{-1} \text{ s}^{-1}\right] \end{cases} \quad (32)$$

where χ represents the solar elevation and Cld is the cloud coverage. More sophisticated models for the photolysis rate k_1 can be found in the literature. These are however generally unfit for operational purposes (Seinfeld, 1986).

6.2. Wet deposition

Wet deposition phenomena are parametrised by means of a wash-out rate factor, referred to as Λ (s^{-1}). Assuming that the wash-out of a pollutant species by a water droplet is irreversible, the flux of pollutant wash-out can be expressed by integrating the particle absorption along the vertical (Slinn, 1984):

$$\Phi_d(x,y) = \int_{z=0}^{+\infty} \Lambda \cdot c(x,y,z)dz \tag{33}$$

In order to take into account these effects on a plume dispersing in the atmosphere, the effect of wash-out can be modelled by a time-varying pollutant emission rate by an ‘effective pollutant flow rate after wash-out’:

$$Q_{S,\mathrm{eff}}(t) = Q_S \exp(-\Lambda t) \tag{34}$$

Similarly, by applying (33) to the volume of the street, the wash-out flux Q_{wash} in (37) can be expressed as:

$$Q_{\mathrm{wash}} = \Lambda \cdot HWL \cdot C_{\mathrm{street}} \tag{35}$$

The wash-out rate depends on the intensity of precipitations, referred here as Pr and expressed in (mm h^{-1}), according to the following relation (Jylha, 1991):

$$\Lambda = a \cdot Pr^b \tag{36}$$

where a and i are constants which depend on the pollutant species. As a first approximation, in the present version of SIRANE, it is assumed that $a = 10^{-4}$ h mm^{-1} s^{-1} and $b = 1$ for all pollutant species.

7. Numerical resolution

The mass balance within the street i can be finally expressed as

$$Q_{S,i} + Q_{I,i} + = \frac{\sigma_w WL}{\sqrt{2\pi}}\left(C_{\mathrm{street},i} - C_{\mathrm{street,ext},i}\right) + HWU_{\mathrm{street}} C_{\mathrm{street},i} + \Lambda \cdot HWL \cdot C_{\mathrm{street}} \tag{37}$$

where $Q_{I,i}$ is the pollutant flux entering the street from the upwind intersection, computed from equation (8). Equation (37) represents the first equation of a coupled system. The other equations that complete the system are those referred to the mass balance in the street intersections (equation (8)) and two other relations given by a sum of Gaussian plumes of the form of equation (23). These provide the concentrations above each street and intersections, referred to as $C_{\mathrm{ext},i}$ and $C_{\mathrm{ext-int},I}$ respectively.

Assuming that H, W and U_{street} are known, we dispose of four coupled linear equations, where the unknown factors are:

- The concentration $C_{\mathrm{street},i}$ in the street i.
- The concentration $C_{\mathrm{ext},i}$ above the street i.
- The convective flux $Q_{E,i}$ entering in the street i by the upwind edge.
- The concentration $C_{\mathrm{ext-int},i}$ above the intersection i.

The problem can then be formalised by a matrix equation:

$$A \cdot x = b$$

where x represents a vector whose components are the unknown factors of the problem. Defined as N_R and N_I the numbers denoting streets and intersections, the linear system is then composed by $3N_R + N_I$ equations with $3N_R + N_I$ unknowns. When a district with lateral dimension of about 1 km is considered, N_R and N_I can be larger than 100 and the size of matrix A becomes very large. It is then difficult to apply exact methods to solve the linear system (e.g. LU factorization). Therefore an iterative Gauss–Seidel method is adopted. In order to improve the convergence of the method, the matrix A is ordered depending on the wind direction, since the concentration within any street a point depends only on the sources located upstream. In this way the iteration needed to obtain a converged solution are reduced of about 30% compared to a resolution of the disordered system.

8. Short-comings of the model

It is worth noting that, in its present version, SIRANE does not provide any specific module for concentration calculation in case of low wind conditions, which are therefore critical for pollutant dispersion modelling, as in most dispersion models. In order to summarise the other main limitations of the model we refer the three geometrical length scales defined in Section 3.

Topography scale ($L > 100$ m)

SIRANE assumes that the wind field in the atmospheric boundary layer is uniform in the horizontal plane and neglects the presence of a roughness sub-layer above roof level. This limits the size of the domain for the application of the model, which is also restraint to the case of districts over flat or almost flat terrain.

Building scale ($L \sim 10$ m)

The model SIRANE was conceived to simulate pollutant dispersion in a street network with a high density of buildings. In these cases the flow fields within the canopy and that in the overlying atmospheric flow appear decoupled (Salizzoni, 2006). Therefore a simple parametrisation of the turbulent mass exchanges based on a box model is able to provide reliable results.

This approach fails when the density of the buildings is lower, in case of streets partially border by buildings or within large squares. In all this cases the flow patterns are significantly more complex (Salizzoni, 2006) than that observed within and highly packed groups of buildings, and the flow within the canopy shows a higher interaction with that in the external atmospheric flow. Further development of the model may therefore include a parameterisation of mass exchange velocity street-atmosphere depending on the street aspect ratio, an exchange model for streets partially bordered by buildings and for pollutant exchange within large squares, that are both designated as open terrain regions in the present version of the model.

Details of building geometry ($L \sim 1$ m)

SIRANE does not include any direct information at a scale smaller than that of the building scale. As an output, SIRANE provides an averaged value of pollutant concentration over the whole volume of the street canyon. Further improvement of the model would require the coupling of SIRANE with a street canyon model providing non uniform spatial distribution of the pollutant within the street due to the characteristic recirculating wind component in the street (Soulhac and Perkins, 2000). Similarly, the model does not provide the spatial distribution of pollutant within street intersections. The intersection are modelled as nodes in the SIRANE network and do not have any physical dimension.

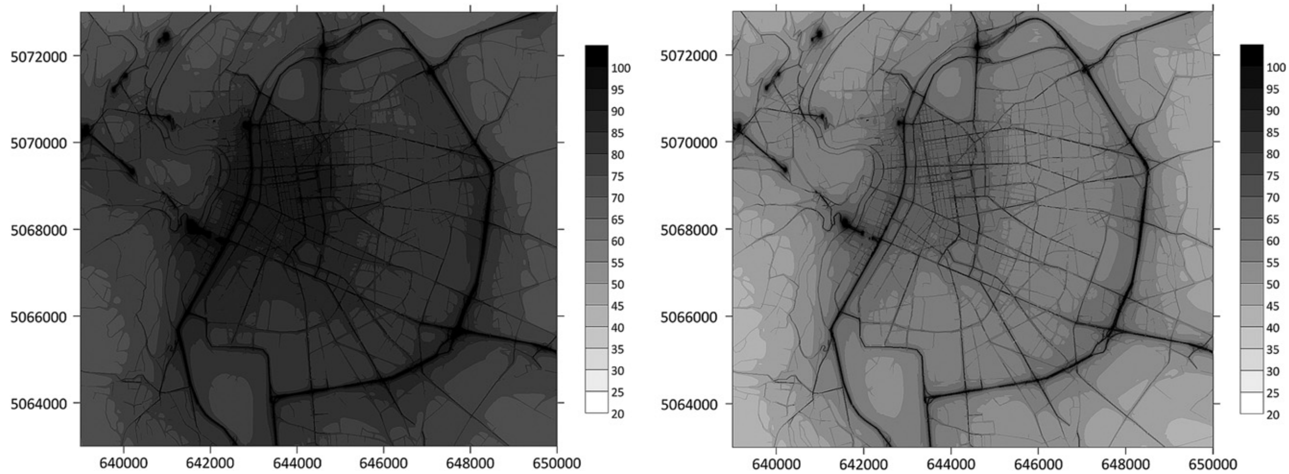

Fig. 13. Example of the pollution cartographies computed with SIRANE over the whole urban area of Lyon (concentrations are expressed in μg m^{-3}).

9. Validation of the model and future development

SIRANE has already been used to compute street level concentrations in several large European cities. These include Paris, Grenoble, Le Havre, Rouen, Chambery and Lyon (Soulhac et al., 2003) where SIRANE is currently adopted by public Authorities as operational tool for air quality management and Turin, Milan, Florence (Garbero et al., 2010; Biemmi et al., 2010; Giambini et al., 2010). An example of the pollution cartographies obtained with SIRANE over the city of Lyon is shown in Fig. 13.

Detailed validations of the model have been performed and will be published shortly. These concern:

- a field validation in an urban district of Lyon (which is presented in the part II of this study) analysing the sensitivity of the model to traffic emissions, meteorological data and geometrical data of the street network (Soulhac et al., submitted for publication);
- a validation against wind tunnel results on an idealised urban geometry (Garbero, 2008) to test the parametrisation of the dispersion phenomena implemented in SIRANE;
- a validation against wind tunnel results in a small scale model of a real urban district (Carpentieri et al., 2009).

Some of the shortcomings of the model presented in Section 8 will be overcome in future versions. These will mainly concern the possibility of taking into account a three-dimensional wind field. It will therefore be possible to perform simulations over larger domains, for example a whole urban area, taking into account the non uniformity of the atmospheric conditions above the urban canopy due to topographic effects.

A further version of the code for unsteady pollutant emissions has been developed. This new model, named SIRANERISK, is conceived in order to provide estimates of the mean and standard deviation of the concentration of a passive scalar emitted during an accidental release within an urban district. To that purpose, it couples the pollutant dispersion model within the urban canopy with a Gaussian puff model for the outer atmosphere. The model provides estimates of mean and standard deviation of pollutant concentration by combining a Gaussian puff model and semi-empirical relations for the intensity of the fluctuations (Cierco et al., 2010).

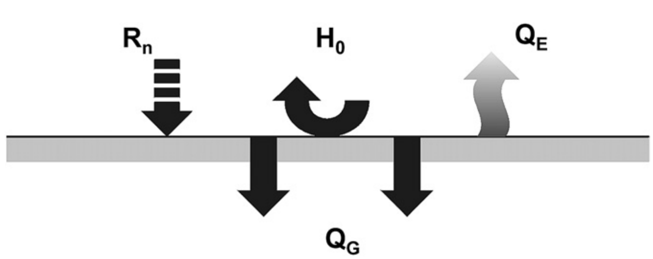

Fig. 14. Energy balance at ground level in steady conditions; we consider that the net radiation R_n and the diffusive heat flux towards the ground Q_G are positive when directed downwards and that the sensible heat flux H_0 and the latent heat flux Q_E are positive when directed upwards.

10. Conclusions

In this paper we have presented the SIRANE model, for atmospheric urban pollutant dispersion, which adopts a simplified description of the urban canopy and a parametrisation of the pollutant transfer phenomena within and above it. The external flow is described assuming self-similar relations for the mean and standard deviation of the three velocity components. The dispersion in this external flow is determined by a simple Gaussian model. To model flow and dispersion within the urban canopy, SIRANE adopts the street network approach: the streets in a district are modelled as a network of street segments connected by nodes that represent intersections. Each street segment is represented by a box: a mass balance within the box is conducted, taking into account inward and outwards fluxes as well as the strength of pollutant sources placed within it.

SIRANE was conceived in order to simulate the main phenomena characterising the transport of pollutant at the district scale:

- Street canyon phenomena (retention of pollutant within recirculating flow regions within the urban canopy)
- Pollutant transfer within street intersection
- Transport in the urban boundary layer above roof level
- Simple chemical reactions (Chapman cycle $NO{-}NO_2{-}O_3$)
- Particle transport (not presented here)
- Wet deposition.

SIRANE is an operational tool, which can treat a large variety of situations, rapidly, and with limited computing resources in order to investigate the effect of air pollution in urban area, and namely to:

- Produce pollution cartography at the district scale, complementary to direct measurements of monitoring stations
- Evaluate the reliability of direct measurements
- Estimate of the exposure of the population to air pollution
- Evaluate the impact of new urban plans, traffic plans or policies for road traffic emission reduction
- Forecast pollution.

The model, which has been validated against wind tunnel experiments and field measurements campaigns, is currently adopted in several European cities as operational tools for air quality management.

Appendix. Estimate of the sensible heat flux in SIRANE's meteorological pre-processor

The sensible heat flux H_0 between earth surface and atmosphere can be directly measured by means of a sonic anemometer. However, for pollution dispersion studies this information is rarely available. Therefore H_0 has to be estimated indirectly by means of an energy balance at ground. Assuming stationary conditions and homogeneity over the earth surface this balance writes (Fig. 14):

$$R_N = H_0 + Q_E + Q_G \quad \text{(A1)}$$

where R_N is the net radiation, Q_E the latent heat flux and Q_G is the diffusive heat flux towards the ground. In case that these parameters are not measured directly, they are modelled as follows:

Net radiation R_N

$$R_N = \underbrace{K_\downarrow}_{\text{Incident short wave}} - \underbrace{K_\uparrow}_{\text{Reflected short wave}} + \underbrace{L_\downarrow}_{\text{Incident long wave}} - \underbrace{L_\uparrow}_{\text{Reflected long wave}} \quad \text{(A2)}$$

The models for the different terms needed to compute the net radiation are given in the relations (A3)–(A6). The incident solar flux is (Kasten and Czeplak, 1980):

$$K_\downarrow = \begin{cases} (990\sin(\psi) - 30)\left(1 - 0.75\left(\dfrac{\text{Cld}}{8}\right)^{3.4}\right) & \text{day}(\sin(\psi)>0) \\ 0 & \text{night}(\sin(\psi)<0) \end{cases}$$
$$\text{with} \begin{cases} \sin(\psi) = \sin(\phi)\sin(\delta) + \cos(\phi)\cos(\delta)\cos\left[\dfrac{2\pi}{24}(t_{HTU} - 12)\right] = \text{solar elevation} \\ \delta = 23.45\sin\left[\dfrac{2\pi}{365}(j + 284)\right] \end{cases} \quad \text{(A3)}$$

where j is the day number (from 1 to 366), t_{HTU} is the local hour, ϕ the site latitude and Cld is the cloud coverage index (octas). The reflected solar radiation is:

$$K_\uparrow = aK_\downarrow \quad \text{(A4)}$$

where a is the albedo of the district which is assumed to be equal to 0.18, as suggested by Stull (1988). The infrared radiative flux emitted by clouds and atmosphere is estimated as (Swinbank, 1963; Holtslag and Van Ulden, 1983):

$$L_\downarrow = L_{\downarrow atm} + L_{\downarrow cloud} = 0.94.10^{-5}\sigma T_0^6 + 60(\text{Cld}/8) \quad \text{(A5)}$$

whereas the infrared radiative flux emitted by the earth surface is (Holtslag and Van Ulden, 1983):

$$L_\uparrow = \varepsilon\sigma T_0^4 + 0.12R_N \quad \text{(A6)}$$

where ε is the district emissivity, assumed to be 0.88 (Stull, 1988). Substituting equations (A3)–(A6) in (A2), we obtain the following relation for the net radiation:

$$R_N = \frac{(1-a)K_\downarrow + \left(0.94\cdot10^{-5}T_0^2 - \varepsilon\right)\sigma T_0^4 + 60(\text{Cld}/8)}{1.12} \quad \text{(A7)}$$

Latent heat flux Q_E

Following Priestley and Taylor (1972) and Holtslag and Van Ulden (1983), the latent heat flux is estimated as:

$$Q_E = \alpha\frac{1}{1+\gamma/s}(R_N - Q_G) + 20\alpha \quad \text{(A8)}$$

with $\frac{s}{\gamma} = \exp[0.055(T_0 - 279)]$ (Van Ulden and Holtslag, 1985) and where α is the Priestley–Taylor coefficient, which depends on the soil saturation rate and on the presence of vegetation ($\alpha = 0 \rightarrow$ dry ground; $\alpha = 1 \rightarrow$ wet ground with vegetation. SIRANE computes the Priestley–Taylor coefficient as follow:

$$\alpha_{\text{dry}} = 1.0\lambda_{\text{veg}} \quad \text{(A9)}$$

where λ_{veg} is the rate of the surface of the district covered by vegetation. In case of precipitations SIRANE impose $\alpha = 1$ and $\alpha = \max(\alpha_{\text{dry}}; 0.45)$ for the first hourly time step after the rain, in order to take into account the presence of water on the ground and on the building walls (De Haan, 1999).

Heat flux in the ground Q_G

De Bruin and Holtslag (1982) suggest to estimate the heat flux towards the ground as a function of the net radiation:

$$Q_G = c_G R_N \quad \text{(A10)}$$

In urban areas, Hanna and Chang (1992) adopt $c_G = 0.3$.

Sensible heat flux H_0

Substituting equations (A8)–(A10) in equation (A1) we finally obtain that:

$$H_0 = \frac{1+(1-\alpha)s/\gamma}{1+s/\gamma}0.7R_N - 20\alpha \tag{A11}$$

References

Barlow, J.F., Dobre, A., Smalley, R.J., Arnold, S.J., Tomlin, A.S., Belcher, S.E., 2009. Referencing of street-level flows measured during the DAPPLE 2004 campaign. Atmospheric Environment 43, 5536–5544.

Batchvarova, E., Gryning, S.-E., 1991. Applied model for the growth of the daytime mixed layer. Boundary-Layer Meteorology 56, 261–274.

Biemmi, S., Gaveglio, R., Salizzoni, P., Boffadossi, M., Casadei, S., Bedogni, M., Garbero, V., Soulhac, L., 2010. Estimate of boundary layer parameters and background concentrations for pollutant dispersion modeling in urban areas. In: 31st NATO/SPS International Technical Meeting on Air Pollution Modelling and its Application, 27 Sep–01 Oct, 2010, Torino, Italy.

Briggs, G.A., 1973. Diffusion Estimation for Small Emissions. Atmospheric Turbulence and Diffusion Laboratory.

Briggs, G.A., 1984. Plume rise and buoyancy effects. In: Atmospheric Science and Power Production NTIS report.

Buccolieri, R., Gromke, C., Di Sabatino, S., Ruck, B., 2009. Aerodynamic effects of trees on pollutant concentration in street canyons. Science of the Total Environment 407, 5247–5256.

Businger, J.A.n, Wyngaard, J.C., Izumi, Y., Bradley, E.F., 1971. Flux-profile relationships in the atmospheric surface layer. Journal of Atmospheric Sciences 28 (2), 181–189.

CERC, 2001. ADMS-Urban User Guide. Cambridge Environmental Research Consultants.

Cai, X.-M., Barlow, J.F., Belcher, S.E., 2008. Dispersion and transfer of passive scalars in and above street canyons-large-eddy simulations. Atmospheric Environment 42, 5885–5895.

Carpintieri, M., Robins, A., 2010. Tracer flux balance at street intersection. Boundary-Layer Meteorology 135, 229–242.

Carpentieri, M., Salizzoni, P., Robins, A., Soulhac, L., 2009. Validation of the neighbourhood scale dispersion model through comparison with wind tunnel data. In: Proceedings of the Conference on Physical Modelling of Flow and Dispersion Phenomena Physmod Conference, Rhode Saint-Genese, Belgium.

Cierco, F.X., Soulhac, L., Méjean, P., Lamaison, G., Salizzoni, P., Armand, P., 2010. SIRANERISK: an operational dispersion model for urban areas incorporating a new method to account for concentration fluctuations. In: 13th International Conference on Harmonisation Within Atmospheric Dispersion Modelling for Regulatory Purposes, Paris, France, 1–4 June 2010.

Christen, A., van Gorsel, E., Vogt, R., 2007. Coherent Structures in an urban roughness sublayer turbulence. International Journal of Climatology 27, 1955–1968.

De Bruin, H.A.R., Holtslag, A.A.M., 1982. A simple parameterization of the surface fluxes of sensible and latent heat during daytime compared with the Penman–Monteith concept. Journal of Applied Meteorology 21, 1610–1621.

De Haan, P., 1999. Studies on short-range air pollution modeling. Thèse de Doctorat, Swiss Federal Institute of Technology Zurich.

Dobre, A., Arnold, S., Smalley, R., Boddy, J., Barlow, J., Tomlin, A., Belcher, S.E., 2005. Flow field measurements in the proximity of an urban intersection in London, UK. Atmospheric Environment 39, 4647–4657.

Duchenne, C., Armand, P., 2010. Development of a 3D modeling suite from the global scale to the urban scale using MM5 and Micro-Swift-Spary. Application to the dispersion of a toxic release in New York City. In: 13th International Conference on Harmonisation Within Atmospheric Dispersion Modelling for Regulatory Purposes, Paris, France, 1–4 June 2010.

Fisher, B.E.A., Erbrink, J.J., Finardi, S., Jeannet, P., Joffre, S., Morselli, M.G., Pechinger, U., Seibert, P., Thomson, D.J., 1998. Harmonisation of the Preprocessing of Meteorological Data for Atmospheric Dispersion Models. COST Action 710 – Final report.

Flaherty, J.E., Stock, D., Lamb, B., 2007. Computational fluid dynamic simulations of plume dispersion in urban Oklahoma city. Journal of Applied Meteorology and Climatology 46, 2110–2126.

Garbero, V., 2008. Pollutant Dispersion in the Urban Canopy. PhD Thesis, Politecnico di Torino – Ecole Centrale de Lyon, 153 pp.

Garratt, J.R., 1992. The atmospheric boundary layer. Cambridge Atmospheric and Space Science Series.

Garbero, V.P., Salizzoni, P., Berrone, S., Soulhac, L., 2010. Air pollution modelling at the urban scale and population exposure: a case study in Turin. In: 31st NATO/SPS International Technical Meeting on Air Pollution Modelling and Its Application, 27 Sep–01 Oct, 2010, Torino, Italy.

Giambini, P., Salizzoni, P., Soulhac, L., Corti, A., 2010. Influence of meteorological input parameters on urban dispersion modeling for traffic scenario analysis. In: 31st NATO/SPS International Technical Meeting on Air Pollution Modelling and Its Application, 27 Sep–01 Oct, 2010, Torino, Italy.

Gomes, M.S.P., Isnard, A.A., Pinto, J.M.C., 2007. Wind tunnel investigation on the retention of air pollutants in three-dimensional recirculation zones in urban areas. Atmospheric Environment 41, 4949–4961.

Grimmond, C.S.B., Oke, T.R., 1999. Aerodynamic properties of urban areas derived from analysis of surface form. Journal of Applied Meteorology 38, 1262–1292.

Hanna, S.R., Chang, J.C., 1992. Boundary-layer parametrizations for applied dispersion modeling over urban areas. Boundary-Layer Meteorology 58, 229–259.

Hanna, S.R., Brown, M.J., Camelli, F.E., Chan, S.T., Coirier, W.J., Hansen, O.R., Huber, A.H., Kim, S., Reynolds, M., 2006. Detailed simulations of atmospheric flow and dispersion in downtown Manhattan, an application of five computational fluid dynamics models. Bulletin of American Meteorological Society, 1713–1726.

Hertel, O., Berkowicz, R., 1989. Modelling pollution from traffic in a street canyon. Evaluation of data and model developement. Tech. rep., DMU Luft A-129, NERI.

Holtslag, A.A.M., Van Ulden, A.P., 1983. A simple scheme for daytime estimates of the surface fluxes from routine weather data. Journal of Climate and Applied Meteorology 22 (4), 517–529.

Hoydysh, W.G., Dabberdt, W.F., 1988. Kinematics and dispersion characteristics of flows in asymmetric street canyons. Atmospheric Environment 22, 2677–2689.

Hunt, J.C.R., Holroyd, R.H., Carruthers, D.J., 1988. Preparatory Studies for a Complex Dispersion Model. CERC Report HB9/88.

Jylha, K., 1991. Empirical scavenging coefficient of radioactive substance released from Chernobyl. Atmospheric Environment 25, 263–270.

Kasten, F., Czeplak, G., 1980. Solar and terrestrial radiation dependent on the amount and type of cloud. Solar Energy 24, 177–189.

Kastner-Klein, P., Fedorovich, E., Rotach, M.W., 2004. Mean flow and turbulence characteristics in an urban roughness sub-layer. Boundary-Layer Meteorology 111, 55–84.

Kim, J., Baik, J., 2003. Effects of inflow intensity on flow and pollutant dispersion in an urban street canyon. Journal of Wind Engineering and Industrial Aerodynamics 91, 309–329.

Luhar, A.K., Britter, R.E., 1989. A random walk model for dispersion in inhomogeneous turbulence in a convective boundary layer. Atmospheric Environment 23, 1911–1924.

McHugh, C.A., Carruthers, D.J., Edmunds, H.A., 1997. Adms-urban: an air quality management system for traffic, domestic and industrial pollution. International Journal of Environment and Pollution 8, 666–674.

Namdeo, A.K., Colls, J.J., 1996. Development and evaluation of sbline, a suite of models for the prediction of pollution concentrations from vehicles in urban areas 189–90, 311– 320.

Nieuwstadt, F.T.M., Tennekes, H., 1981. A rate equation for the nocturnal boundary layer height. Journal of the Atmospheric Sciences 38, 1418–1428.

Offerle, B., Eliasson, I., Grimmond, C., Holmer, B., 2007. Surface heating in relation to air temperature, wind and turbulence in an urban street canyon. Boundary-Layer Meteorology 122, 273–292.

Pasquill, F., Smith, F.B., 1983. Atmospheric Diffusion, third ed. John Wiley & Sons.

Priestley, C.H.B., Taylor, R.J., 1972. On the assessment of surface heat flux and evaporation using large-scale parameters. Monthly Weather Review 100 (2), 81–92.

Raupach, M.R., Thom, A.S., Edwards, I., 1980. A wind-tunnel study of turbulent flow close to regularly arrayed rough surfaces. Boundary-Layer Meteorology 18, 373–397.

Rotach, M.W., 1993. Turbulence close to an urban surface. Part I: Reynolds stress. Boundary-Layer Meteorology 65, 1–28.

Roth, M., 2000. Review of atmospheric turbulence over cities. Quarterly Journal of the Royal Meteorological Society 126, 941–990.

Seinfeld, J.H., 1986. Atmospheric Chemistry and Physics of Air Pollution. John Wiley & Sons.

Sini, J.-F., Anquentin, S., Mestayer, P., 1996. Pollutant dispersion and thermal effects in urban street canyons. Atmospheric Environment 30 (15), 2659–2677.

Slinn, W.G.N., 1984. Precipitation scavenging. In: Atmospheric Science and Power Production NTIS report.

Salizzoni, P., 2006. Mass and momentum transfer in urban boundary layer. PhD Thesis, Politecnico di Torino – Ecole Centrale de Lyon.

Salizzoni, P., Soulhac, L., Mejean, P., Perkins, R.J., 2008. Influence of a two scale surface roughness on a turbulent boundary layer. Boundary-Layer Meteorology 127 (1), 97–110.

Salizzoni, P., Soulhac, L., Mejean, P., 2009a. Street canyon ventilation and atmospheric turbulence. Atmospheric Environment 43, 5056–5067.

Salizzoni, P., Van Liefferinge, R., Soulhac, L., Mejean, P., Perkins, R.J., 2009b. Influence of wall roughness on the dispersion of a passive scalar in a turbulent boundary layer. Atmospheric Environment 43 (3), 734–748.

Singh, B., Hansen, B.S., Brown, M.J., Pardyjak, E.R., 2008. Evaluation of the QUIC-URB fast response urban wind model for a cubical building array and wide building street canyon. Environmental Fluid Mechanics 8, 281–312.

Soulhac, L., 2000. Modélisation de la dispersion atmosphérique à l'intérieur de la canopée urbaine. Thèse de doctorat, Ecole Centrale de Lyon.

Soulhac, L., Perkins, R.J., 2000. A new model for flow and dispersion in a street-canyon. Air Pollution Modelling and Its Application 13, 475–483.

Soulhac, L., Puel, C., Duclaux, O., Perkins, R.J., 2003. Simulations of atmospheric pollution in Greater Lyon an example of the use of nested models. Atmospheric Environment 37, 5147–5156.

Soulhac, L., Perkins, R.J., Salizzoni, P., 2008. Flow in a street canyon for any external wind direction. Boundary-Layer Meteorology 126, 365–388.

Soulhac, L., Garbero, V., Salizzoni, P., Mejean, P., Perkins, R., 2009. Flow and dispersion in street intersections. Atmospheric Environment 43, 2981–2996.

Soulhac, L., Salizzoni, P., Perkins, R.J. The model SIRANE for atmospheric urban pollutant dispersion: Part II, validation of the model on a case study. Atmospheric Environment, submitted for publication.

Stull, R.B., 1988. An Introduction to Boundary Layer Meteorology. Kluwer Academic Publishers.

Swinbank, W.C., 1963. Longwave radiation from clear skies. Quarterly Journal of Royal Meteorology Society 89, 339–348.

Tomlin, A.S., Smalley, R.J., Tate, J.E., Barlow, J.F., Belcher, S.E., Arnold, S.J., Dobre, A., Robins, A., 2009. A field study of factors influencing the concentrations of a traffic-related pollutant in the vicinity of a complex urban junction. Atmospheric Environment 43, 5027–5037.
Trini Castelli, S., Morelli, S., Anfossi, D., Carvalho, J., Zauli Sajani, S., 2004. Intercomparison of two models, ETA and RAMS, with TRACT field campaign data. Environmental Fluid Mechanics 4, 157–196.
Vachon, P., Louka, G., Rosant, J.M., Mestayer, P., Sini, J.-F., 2002. Measurements of traffic induced turbulence within a street canyon during the Nantes '99 experiment. Water, Air, and Soil Pollution: Focus 2 (127), 140.
Van Ulden, A.P., Holtslag, A.A.M., 1985. Estimation of atmospheric boundary layer parameters for diffusion applications. Journal of Climate and Applied Meteorology 24, 1196–1207.
Venkatram, A., 1992. Vertical dispersion of ground-level releases in the surface boundary layer. Atmospheric Environment 26 (5), 947–949.
Weil, J.C., 1985. Updating applied diffusion models. Journal of Climate and Applied Meteorology 24 (11), 1111–1130.
Yamartino, R.J., Wiegand, G., 1986. Development and evaluation of simple models forthe flow, turbulence and pollutant concentration fields within an urban street canyon. Atmospheric Environment 20 (11), 2137–2156.